Indeed ferromagnetic coupling between gadolinium(III) and copper(II) is possible only through a superexchange interaction mediated by the bridging oxygen ligands. In other words the magnetic orbitals centered on Gd and Cu must have a fairly large overlap density on the oxygen atom,[49] which can be obtained only through a fairly substantial covalency of the Gd–O bond.

Finally we would like to observe that ferromagnetic exchange, which up to now has been regarded as quite uncommon,[50] is indeed now rather frequently observed,[30,51-53] presumably because many compounds containing different metal ions are being studied, or even in compounds containing one type of metal ion the interactions involving the ground and excited states are actively investigated.[37,54,55]

Further studies are in progress involving other lanthanides and different stoichiometries in order to get a deeper insight into this exciting field of magnetic interactions.

Supplementary Material Available: Tables of positional parameters for hydrogen atoms and thermal parameters for both compounds and observed and calculated structure factors (62 pages). Ordering information is given on any current masthead page.

(47) Linares, C.; Lonat, A.; Blanchard, M. *Struct. Bonding (Berlin)* 1977, *33*, 174.

(48) Sinha, S. P. *Struct. Bonding (Berlin)* 1976, *25*, 69.

(49) Kahn, O.; Charlot, M. F. *Nouv. J. Chim.* 1980, *4*, 567.

(50) Stevens, K. W. H. In "Magneto-Structural Correlation in Exchange Coupled Systems", Willet, R. D., Gatteschi, D., Kahn, O., Eds.; Reidel: Dordrecht, Netherlands, 1985; p 57.

(51) Kahn, O. In "Magneto-Structural Correlation in Exchange Coupled System"; Willet, R. D., Gatteschi, D., Kahn, O., Eds.; Reidel: Dordrecht, Netherlands, 1985; p 57.

(52) Journaux, Y.; Kahn, O.; Zarembovitch, J.; Jand, J. *J. Am. Chem. Soc.* 1983, *105*, 7585.

(53) Kahn, O.; Galj, J.; Journaux, Y.; Morgenstern-Badarau, I. *J. Am. Chem. Soc.* 1982, *104*, 2165. See also the discussion in Chapter 9 of the following: Carlin, R. L. "Magnetochemistry"; Springer-Verlag: Berlin, Heidelberg, New York, Tokyo, 1985.

(54) Banci, L.; Bencini, A.; Gatteschi, D. *J. Am. Chem. Soc.* 1983, *105*, 761.

(55) Bencini, A.; Benelli, C.; Gatteschi, D.; Zanchini, D. *J. Am. Chem. Soc.* 1984, *106*, 5813.

Systematics of the Formation of II-CO Ligands in Four-Iron Clusters. Synthesis and Structures of [K(18-crown-6)][Fe$_4$(AuPEt$_3$)(CO)$_{13}$]·CH$_2$Cl$_2$, Fe$_4$(AuPEt$_3$)(CO)$_{12}$(COCH$_3$), [PPN][Fe$_4$(CuPPh$_3$)(CO)$_{13}$], and [PPN][Fe$_4$(HgCH$_3$)(CO)$_{13}$]

Colin P. Horwitz,[1a] **Elizabeth M. Holt,**[*1b] **Carolyn P. Brock,**[*1a,c] and **Duward F. Shriver**[*1a]

Contribution from the Departments of Chemistry, Northwestern University, Evanston, Illinois 60201, and Oklahoma State University, Stillwater, Oklahoma 74078. Received July 3, 1985

Abstract: The Lewis acid ligands [R$_3$PAu]$^+$, [LCu]$^+$, and [CH$_3$Hg]$^+$ interact with the metal framework of the tetrahedral iron cluster [Fe$_4$(CO)$_{13}$]$^{2-}$. In all cases, two products result, one of which consists of the Fe$_4$ tetrahedron with the Lewis acid capping one face. The other more novel product is a Fe$_4$ butterfly array with the Lewis acid ligand on the hinge and a II-CO between the wingtips. By proper choice of counterion and conditions, either the butterfly or tetrahedral form can be crystallized. X-ray structures were determined for representative compounds of both products in this series. Tetrahedral iron frameworks were observed for [PPN][Fe$_4$(CuPPh$_3$)(CO)$_{13}$] (**5a**) and [PPN][Fe$_4$(HgCH$_3$)(CO)$_{13}$] (**6**(tetrahedron)). Both [K(18-crown-6)][Fe$_4$(AuPEt$_3$)(CO)$_{13}$]·CH$_2$Cl$_2$ (**3a**) and Fe$_4$(AuPEt$_3$)(CO)$_{12}$(COCH$_3$) (**7**) have butterfly iron cores. Butterfly complexes such as **3a** display a characteristic and unique low-frequency II-CO stretch in the 1380–1430-cm^{-1} region of the IR spectrum. Additionally, NMR spectra of the individual isomers were obtained by dissolving the pure crystalline material at −80 °C and obtaining the spectrum at this temperature. The NMR spectra obtained in this manner were consistent with both IR spectra of the solid and the structure determined by X-ray crystallography.

The cleavage of CO on a metal such as Fe, Ru, or Ni is strongly implicated as a key step in Fischer–Tropsch and methanation catalysts.[2] It is thought that this reaction proceeds through a C- and O-bonded carbonyl,[3] −CO I, a point which is logical but speculative.[4] In keeping with this interpretation, experiments on alloy catalysts suggest that for the methanation reaction a minimum ensemble of several metal atoms is necessary for CO cleavage.[5] The II-CO ligand also is strongly implicated in the

(1) (a) Northwestern University. (b) Oklahoma State University. (c) On leave from University of Kentucky, Lexington, Kentucky, 40506.
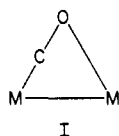
(2) Biloen, P.; Sachtler, W. M. H. *Adv. Catal.* 1981, *30*, 165.

(3) Horwitz, C. P.; Shriver, D. F. *Adv. Organomet. Chem.* 1984, *23*, 219.

(4) Sachtler, W. M. H.; Shriver, D. F.; Hollenberg, W. B.; Lang, A. F. *J. Catal.* 1985, *92*, 429.

(5) (a) Araki, M.; Ponec, V. *J. Catal.* 1976, *44*, 439. (b) Bond, G. C.; Turnham, B. D. *Ibid.* 1976, *45*, 128.

proton-induced reduction of CO in metal-cluster systems.[6] Despite

the apparent activation of Π-CO clusters, there have been no systematic routes developed for the generation of Π-CO in three-metal systems and larger clusters. The present report describes our success in the formation of Π-CO in organometallic clusters, and the following paper[7] describes some of the chemistry of these species.

In dinuclear complexes of the type $Mn_2(CO)_6(PP)_2$ (where PP is a chelating diphosphine), it has been shown that bulky diphosphine ligands lead to the expulsion of a CO ligand and concomitant formation of a Π-CO.[3,8] Similarly it was postulated that the Π-CO observed in the structure of $[HFe_4(CO)_{13}]^-$ arises from the steric influence of the H ligand.[9] These observations prompted us to explore the synthesis and structure of some highly sterically crowded clusters having the formula $[Fe_3M(CO)_{14}]^{2-}$, M = Cr, Mo, W. It was found that these compounds do not contain Π-CO ligands.[10]

The lack of success with steric induction of Π-CO formation led us to consider electronic factors which might induce the opening of a 60 cluster valence electron (CVE) M_4 tetrahedral cluster to yield an M_4 butterfly. According to the systematics of metal-cluster bonding,[11] the 60-CVE butterfly should be unstable, but if one CO ligand were to adopt a Π-CO configuration, in which CO is a formal 4-electron donor, a stable 62-CVE cluster might result. Indeed the demonstrated influence of a proton on $[Fe_4(CO)_{13}]^{2-}$, eq 1, might be viewed in these terms.[9,12]

(1)
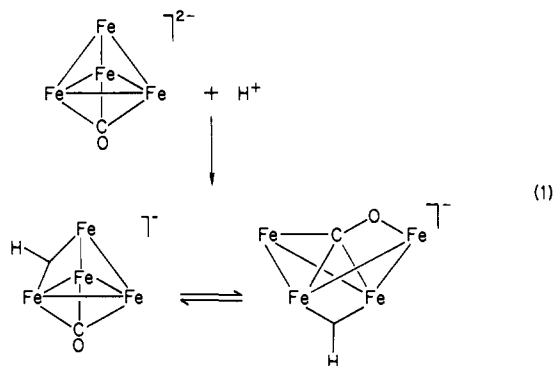
A recent set of MO calculations by Harris and Bradley[13] on related iron clusters provides an indication that protonation may stabilize the butterfly M_4 array. An excerpt from their energy level scheme, Figure 1, reveals that the HOMO, $6a_1$, of the butterfly compound $[Fe_4(CO)_{12}C]^{2-}$ is largely localized on the hinge position and that upon protonation at this site the MO undergoes a large drop in energy. Although this calculation was
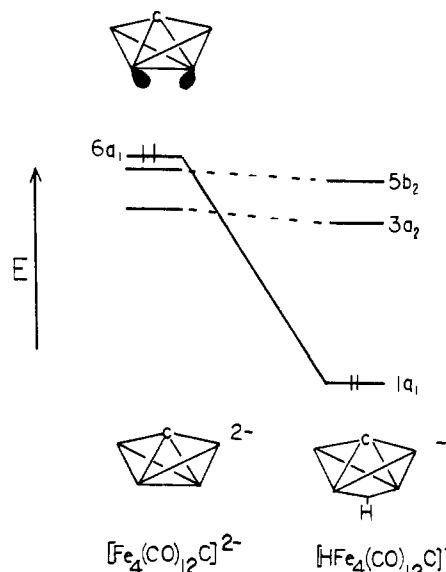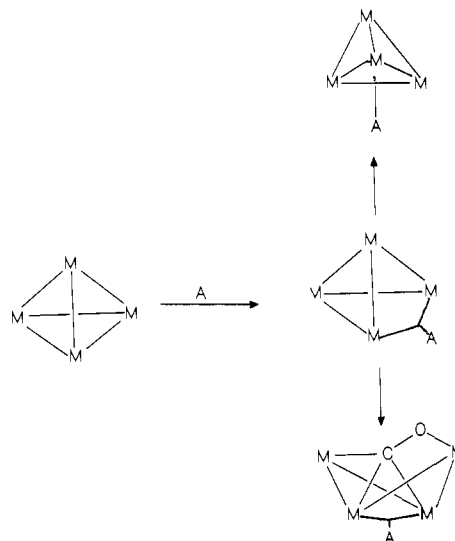

Figure 1. Schematic energy level diagram for $[Fe_4(CO)_{12}C]^{2-}$ and $[HFe_4(CO)_{12}C]^-$. For complete details see ref 13.

Scheme I

not directly addressed to the issue of total energy differences between protonated butterfly and tetrahedral forms, it did prompt us to explore the extent to which general electron acceptors might induce the conversion of tetrahedral $[Fe_4(CO)_{13}]^{2-}$ to the butterfly form containing a Π-CO. A schematic representation of the possible reaction products is shown in Scheme I. The chosen acceptors, R_3PAu^+, LCu^+, and CH_3Hg^+, often mimic the behavior of the proton in their reactions with metal clusters.[14-17] The

(6) (a) Whitmire, K. H.; Shriver, D. F. *J. Am. Chem. Soc.* **1980**, *102*, 1456. (b) Drezdon, M. A.; Whitmire, K. H.; Bhattacharyya, A. A.; Hsu, W. L.; Nagel, C. C.; Shore, S. G.; Shriver, D. F. *Ibid.* **1982**, *104*, 5630.

(7) Horwitz, C. P.; Shriver, D. F. *J. Am. Chem. Soc.*, following paper in this issue.

(8) (a) Colton, R.; Commons, C. J.; Hoskins, B. F. *J. Chem. Soc., Chem. Commun.* **1975**, 363. (b) Wolff, T. E.; Klemann, L. P. *Organometallics* **1982**, *1*, 1667.

(9) (a) Manassero, M.; Sansoni, M.; Longoni, G. *J. Chem. Soc., Chem. Commun.* **1976**, 919. (b) Doedens, R. J.; Dahl, L. F. *J. Am. Chem. Soc.* **1966**, *88*, 4847.

(10) Horwitz, C. P.; Holt, E. M.; Shriver, D. F. *Inorg. Chem.* **1984**, *23*, 2491.

(11) (a) Lauher, J. W. *J. Am. Chem. Soc.* **1978**, *100*, 5305. (b) Wade, K. *Adv. Inorg. Chem. Radiochem.* **1976**, *18*, 1. (c) Mingos, D. M. P. *Nature (London) Phys. Sci.* **1972**, *236*, 99.

(12) Horwitz, C. P.; Shriver, D. F. *Organometallics* **1984**, *3*, 756.

(13) Harris, S.; Bradley, J. S. *Organometallics* **1984**, *3*, 1086.

(14) Evans, D. G.; Mingos, D. M. P. *J. Organomet. Chem.* **1982**, *232*, 171.

(15) (a) Hall, K. P.; Mingos, D. M. P. *Prog. Inorg. Chem.* **1984**, *32*, 237 and references therein. (b) Braunstein, P.; Schubert, U.; Burgand, M. *Inorg. Chem.* **1984**, *23*, 4057. (c) Bruce, M. I.; Nicholson, B. K. *Organometallics* **1984**, *3*, 101. (d) Bunkhall, S. R.; Holden, H. D.; Johnson, B. F. G.; Lewis, J.; Pain, G. N.; Raithby, P. R.; Taylor, M. J. *J. Chem. Soc., Chem. Commun.* **1984**, 25. (e) Carriedo, G. A.; Howard, J. A. K.; Stone, F. G. A.; Went, M. J. *J. Chem. Soc., Dalton Trans.* **1984**, 2545. (f) Green, M.; Orpen, A. G.; Salter, I. D.; Stone, F. G. A. *Ibid.* **1984**, 2497. (g) Braunstein, P.; Rose, J.; Manotti-Lanfredi, A. M.; Tiripicchio, A.; Sappa, E. *Ibid.* **1984**, 1843. (h) Mays, M. J.; Raithby, P. R.; Taylor, P. L.; Henrick, K. *Ibid.* **1984**, 959. (i) Salter, I. D.; Stone, F. G. A. *J. Organomet. Chem.* **1984**, *260*, C71.

(16) (a) Freeman, M. J.; Green, M.; Orpen, A. G.; Salter, I. D.; Stone, F. G. A. *J. Chem. Soc., Chem. Commun.* **1983**, 1332. (b) Heaton, B. T.; Strona, L.; Martinengo, S.; Strumolo, D.; Albano, V. G.; Braga, D. *J. Chem. Soc., Dalton Trans.* **1983**, 2175. (c) Braunstein, P.; Rose, J. *J. Organomet. Chem.* **1984**, *262*, 223.

8138 *J. Am. Chem. Soc., Vol. 107, No. 26, 1985*

Horwitz et al.

interaction of AuPPh$_3^+$ with [Fe$_4$(CO)$_{13}$]$^{2-}$ has been reported[18] but the product was not isolated or structurally characterized. Preliminary results from our present study have been reported.[19]

Experimental Section

Materials and Methods. All manipulations were performed under an atmosphere of prepurified N$_2$ with standard Schlenk techniques. Air-sensitive and toxic solids were manipulated in a Vacuum Atmosphere glovebox under N$_2$. Solvents were distilled under N$_2$ from appropriate drying agents: pentane and Et$_2$O from sodium benzophenone, CH$_2$Cl$_2$ from P$_2$O$_5$ toluene from sodium, and MeOH from Mg activated with I$_2$. Published procedures were used to prepare [PPN]$_2$[Fe$_4$(CO)$_{13}$][20] and [Cu(CH$_3$CN)$_4$][PF$_6$].[21] The K$^+$ salt of [Fe$_4$(CO)$_{13}$]$^{2-}$ was prepared from [Fe(py)$_6$][Fe$_4$(CO)$_{13}$] in MeOH containing 2 equiv of KOH and was crystallized by slow addition of CH$_2$Cl$_2$. The compound K[Fe$_4$-(CO)$_{12}$(COMe)] was prepared by appropriate modification of the procedures for preparation of [PPPn][Fe$_4$(CO)$_{12}$(COMe)].[22] The reagents [(CH$_3$)$_3$O][BF$_4$] (Alfa), PPNCl (Aldrich) [PPN = bis(triphenyl-phosphinenitrogen)(1+)], PPh$_3$AuCl (Strem), PEt$_3$AuCl (Strem), TlPF$_6$ (Strem), CH$_3$HgCl (Strem), HPF$_6$ (Aldrich), PPh$_3$ (Aldrich), and 1,4,7,10,13,16-hexaoxacyclooctadecane (18-crown-6) (Aldrich) were all used as received. The 2,6-dimethylphenyl isocyanide (Alfa) was sublimed prior to use. The [PPN]$_2$[Fe$_4$(CO)$_{13}$] was enriched to approximately 25% ^{13}CO with published procedures.[10] The ^{13}CO-enriched K$_2$[Fe$_4$(CO)$_{13}$], 10% ^{13}CO, was prepared from ^{13}CO-enriched Fe(CO)$_5$.[23] NMR spectra were recorded on either a JEOL FX90Q spectrometer (^{1}H, 89.55 MHz; ^{13}C, 22.49 MHz; ^{31}P, 36.19 MHz; and ^{199}Hg, 15.96 MHz) or a JEOL FX270 spectrometer (^{13}C, 67.80 MHz); ^{31}P spectra were referenced to external 85% H$_3$PO$_4$ and ^{199}Hg spectra were referenced to external 0.15 M CH$_3$HgCl in CDCl$_3$. Both instruments were equipped with varia-ble-temperature controllers. Spectra were obtained in CD$_2$Cl$_2$ (99.5 or 20 atom % D) or (CD$_3$)$_2$CO (99.75 atom % D). Infrared spectra were recorded on either a Perkin-Elmer Model 283 or 399 spectrophotometer. Solution cells with 0.1-mm path lengths and CaF$_2$ windows were used. The spectra of solids were obtained on Nujol or Fluorolube mulls between KBr windows. Analyses were performed by Galbraith Labs, Knoxville, TN or on a Hitachi 180-80AA atomic absorption unit at Northwestern University.

Synthesis of [K(18-crown-6)][Fe$_4$(AuPR$_3$)(CO)$_{13}$] (R = Et (3a) or Ph (3b)). A sample of K$_2$[Fe$_4$(CO)$_{13}$], 150 mg, was dissolved in MeOH (5 mL) and 1 equiv of Et$_3$PAuCl was added. The solution was stirred for 10 min and the MeOH was removed in vacuo. The remaining solid was redissolved in Et$_2$O, (10 mL) and filtered, and Et$_2$O was stripped off at reduced pressure. The solid was redissolved in CH$_2$Cl$_2$ (5 mL) followed by addition of 1 equiv of 18-crown-6. Slow addition of pentane with periodic shaking resulted in formation of a microcrystalline black solid which was recovered by filtration, washed with pentane, and dried in vacuo. The solid is stable for short periods in air but solutions decompose rapidly. The yield of [K(18-crown-6)][Fe$_4$(AuPEt$_3$)(CO)$_{13}$] was 200 mg, 73.5% based on starting K$_2$[Fe$_4$(CO)$_{13}$]. This compound loses the CH$_2$Cl$_2$ of crystallization rapidly, therefore the analysis was calculated for a sample which presumably had lost all CH$_2$Cl$_2$. ^{13}C NMR ((CD$_3$)$_2$CO, -80 °C) ligand and cation resonances: (3a) [K(18-crown-6)]$^+$, 70.4; PCH$_2$CH$_3$, 1.94 d ($^1J_{P-C}$ = 29.3 Hz); PCH$_2$CH$_3$, 8.8 ppm. (3b) [K(18-crown-6)]$^+$, 70.4; PPh$_3$, 134–129 ppm multiplet. Anal. Calcd (Found) for C$_{31}$H$_{39}$PFe$_4$O$_{19}$KAu: Fe, 18.53 (15.06); Au, 16.34 (17.09); C, 30.89 (30.96); H, 3.23 (3.25); P, 2.57 (2.23). When 18-crown-6 was replaced by dibenzo(18-crown-6) or cryptands only only oils

formed on attempted crystallization.

Synthesis of [PPN][Fe$_4$(AuPR$_3$)(CO)$_{13}$] (R = Et (4a) or Pb (4b)). A sample of K$_2$[Fe$_4$(CO)$_{13}$] (100 mg) was combined with PPh$_3$AuCl (90 mg) and MeOH (5 mL) was added. The solution was stirred for 10 min followed by removal of MeOH in vacuo. The solid was redissolved in Et$_2$O and filtered, and the Et$_2$O was removed under reduced pressure. The solid was redissolved in MeOH (3 mL) and [PPN]Cl (1 equiv) was added. Cooling the solution to -20 °C for approopoximately 1–3 days resulted in the formation of black crystalline [PPN][Fe$_4$(AuPPh$_3$)-(CO)$_{13}$], which was recovered by filtration, washed with cold (0 °C) Et$_2$O and dried in vacuo. Attempts to recrystallize this complex resulted in the formation of oils or in the expulsion of AuPR$_3$. The yield of [PPPn][Fe$_4$(AuPPh$_3$)(CO)$_{13}$] was 160 mg, 67% based on starting K$_2$-[Fe$_4$(CO)$_{13}$]. The AuPEt$_3$ derivative is more soluble than the AuPPh$_3$ complex and was isolated in 43% yield. Solutions of this cluster rapidly decompose when exposed to air but the solid is stable for hours in air. ^{13}C NMR (CD$_2$Cl$_2$, -80 °C) ligand and cation resonances: (4a) PCH$_2$CH$_3$, 19.1 d (J_{P-C} = 28 Hz); PCH$_2$CH$_3$, 8.3; [PPN]$^+$ 130 ppm multiplet. (4b) PPh$_3$ and [PPN]$^+$, 130 ppm multiplet. Anal. Calcd (Found) for C$_{67}$H$_{45}$NP$_3$O$_{13}$Fe$_4$Au: C, 50.78; (48.37); H, 2.84 (3.16); P, 5.87 (5.23); Fe, 14.11 (11.67); Au, 12.38 (11.96).

Synthesis of [PPN][Fe$_4$(CuL)(CO)$_{13}$] (L = PPh$_3$ (5a) or 2,6-(CH$_3$)$_2$C$_6$H$_3$NC (5b)). Procedures for the synthesis of both the phosphine and isocyanide complexes are identical so only that for the PPh$_3$ complex is described. A sample of [PPN]$_2$[Fe$_4$(CO)$_{13}$] (250 mg) was combined with [Cu(CH$_3$CN)$_4$][PF$_6$] (60 mg) to which was added CH$_2$Cl$_2$ (5 mL). Dichloromethane which is freshly distilled under N$_2$ is essential for this reaction; less pure solvent produces a Cu mirror. The reaction was allowed to proceed for 10 min and then no more than 5 vol equiv of Et$_2$O were added to precipitate [PPN][PF$_6$], which was removed by filtration. The solvents were removed by vacuum. The solid was redissolved in MeOH and 1 equiv of PPh$_3$ was then added, whereupon crystalline [PPN][Fe$_4$(CuPPh$_3$)(CO)$_{13}$] formed. Addition of excess phosphine displaces the Cu from the cluster and a precipitate of the starting iron cluster results. Analogous results have been observed for MCo$_3$-(CO)$_{12}$(CuPPh$_3$) (M = Fe or Ru) where excess PPh$_3$ forms [Cu-(PPh$_3$)$_3$][MCo$_3$(CO)$_{12}$].[24] The black solid was recovered by filtration, washed with MeOH, and then dried in vacuo. The solid is reasonably air stable but solutions rapidly decompose in air. The yield of [PPN]-[Fe$_4$(CuPPh$_3$)(CO)$_{13}$] was 135 mg, 62% based on starting [PPN]$_2$[Fe$_4$(CO)$_{13}$]. Ligand and cation resonances, ^{13}C NMR (CD$_2$Cl$_2$, -80 °C): (5a) PPh$_3$ and [PPN]$^+$, 130 ppm multiplet. (5b) 2,6-(CH$_3$)$_2$C$_6$H$_3$NC, 18.3; 2,6-(CH$_3$)$_2$CH$_3$NC and [PPN]$^+$, 130 ppm multiplet. ^{1}N NMR (CD$_2$Cl$_2$, -80 °C): (5a) PPh$_3$ and [PPN]$^+$, 7.4 ppm multiplet. (5b) 2,6-(CH$_3$)$_2$C$_6$H$_3$NC, 2.3; 2,6-(CH$_3$)$_2$C$_6$H$_3$NC and [PPN]$^+$, 7.4 ppm multiplet. Anal. Calcd (Found) for C$_{67}$H$_{45}$O$_{13}$P$_3$NFe$_4$Cu: Fe, 15.40 (11.33); Cu, 4.38 (4.12); C, 55.41 (55.30); H, 3.10 (3.67); P, 6.41 (6.50).

Synthesis of [PPN][Fe$_4$(HgCH$_3$)(CO)$_{13}$] (6). A sample of [PPN]$_2$-[Fe$_4$(CO)$_{13}$] (300 mg) was combined with TlPF$_6$ (60 mg) and CH$_3$HgCl (45 mg) to which was added CH$_2$Cl$_2$ (5 mL). The reaction was allowed to proceed for 5 min (significantly longer reaction times results in decomposition) and then 30 mL of Et$_2$O was added to precipitate [PP-N][PF$_6$]. This [PPN][PF] and TlCl was removed by filtration. The solvents were reduced in volume under vacuum until crystalline material was observed to form; then pentane was added slowly to crystallize the remaining product. Crystallization of product in this manner yielded 6(butterfly). If, however, pentane was layered onto the Et$_2$O/CH$_2$Cl$_2$ solution, slow diffusion produced 6(tetrahedron). These isomers could be identified by their significantly different IR spectra. The solid was recovered by filtration, washed with pentane, and dried in vacuo. The yield of [PPN][Fe$_4$(HgCH$_3$)(CO)$_{13}$] (butterfly isomer) was 180 mg, 75% based on starting [PPN]$_2$[Fe$_4$(CO)$_{13}$]. The solid decomposes slowly in air but solutions are very air sensitive. Anal. Calcd (Found) for C$_{50}$H$_{33}$NP$_2$O$_{13}$Fe$_4$Hg(butterfly isomer): C, 44.76 (45.53); H, 2.46 (2.60); P, 4.62 (4.28); Fe, 16.67 (15.29); Hg, 14.92 (14.16).

Synthesis of Fe$_4$(AuPEt$_3$)(CO)$_{12}$(COMe) (7): A sample of K[Fe$_4$-(CO)$_{12}$(COMe)] (50 mg) was combined with PEt$_3$AuCl (1 equiv) and toluene (5 mL) was added. The reaction was allowed to proceed for 30 min and then the toluene was removed in vacuo. The solid was extracted with pentane and filtered, and the pentane was concentrated under vacuum until crystals began to form. Cooling the solution to -20 °C resulted in the crystallization of additional product. The product was recovered by filtration and dried under vacuum, yielding 55 mg, 75%, of Fe$_4$(AuPEt$_3$)(CO)$_{12}$(COMe). ^{1}H NMR (CD$_2$Cl$_2$, -80 °C): COCH$_3$, 4.02 ppm. Anal. Calcd (Found) for C$_{20}$H$_{18}$PO$_{13}$Fe$_4$Au: Fe, 24.34

(17) (a) King, R. B. *J. Inorg. Nucl. Chem.* **1963**, *25*, 1296. (b) Deutscher, J.; Fadd, S.; Ziegler, M. L. *Angew. Chem., Int. Ed. Engl.* **1977**, *16*, 704. (c) Fajardo, M.; Holden, H. D.; Johnson, B. F. G.; Lewis, J.; Raithby, P. R. *J. Chem. Soc., Chem. Commun.* **1984**, 24. (d) Duffy, D. N.; Mackay, K. M.; Nicholson, B. K.; Robinson, W. T. *J. Chem. Soc., Dalton Trans.* **1981**, 381. (e) Statler, J. A.; Wilkinson, G.; Thornton-Pett, M.; Hursthouse, M. B. *Ibid.* **1984**, 1731. (f) Rosenberg, E.; Fahmy, R.; King, K.; Tiripicchio, A.; Camellini, M. T. *J. Am. Chem. Soc.* **1980**, *102*, 3626. (g) Albinati, A.; Moor, A.; Pregosin, P. S.; Venanzi, L. M. *Ibid.* **1982**, *104*, 7672. (h) Yamamoto, Y.; Yamazaki, H.; Sakurai, T. *Ibid.* **1982**, *104*, 2329. (i) Ermer, S.; King, K.; Hardcastle, K. I.; Rosenberg, E.; Manotti-Lanfredi, A. M.; Tiripicchio, A.; Camellini, M. T. *Inorg. Chem.* **1983**, *22*, 1339.

(18) Johnson, B. F. G.; Kaner, D. A.; Lewis, J.; Rosales, M. J. *J. Organomet. Chem.* **1982**, *238*, C73.

(19) Horwitz, C. P.; Holt, E. M.; Shriver, D. F. *J. Am. Chem. Soc.* **1985**, *107*, 281.

(20) Whitmire, K.; Ross, J.; Cooper, C. B., III; Shriver, D. F. *Inorg. Synth.* **1982**, *21*, 66.

(21) Kubas, G. J. *Inorg. Synth.* **1979**, *19*, 90.

(22) (a) Holt, E. M.; Whitmire, K.; Shriver, D. F. *J. Chem. Soc., Chem. Commun.* **1980**, 778. (b) Dawson, P. A.; Johnson, B. F. G.; Lewis, J.; Raithby, P. R. *Ibid.* **1980**, 781.

(23) Noack, K.; Ruch, M. *J. Organomet. Chem.* **1969**, *17*, 309.

(24) Braunstein, P.; Rose, J.; Dedieu, A.; Dusavsoy, Y.; Mangeot, J.; Tiripicchio, A.; Tiripicchio-Camellini, M. *J. Chem. Soc., Dalton Trans.*, submitted.

Table I. Crystal Data for X-ray Diffraction Studies

compound	3a	5a	6 (tetrahedron)	7
formula	$C_{32}H_{41}AuCl_2Fe_4KO_{19}P$	$C_{67}H_{45}CuFe_4P_3NO_{13}$	$C_{50}H_{33}HgFe_4P_2NO_{13}$	$C_{20}H_{18}AuFe_4PO_{13}$
mol wt	1290.99	1451.9	1341.74	917.7
crystal dimens, mm	0.19 × 0.44 × 0.22	0.2 × 0.2 × 0.35	0.07 × 0.23 × 0.37	0.1 × 0.15 × 0.25
space group	*Pnma*	*P*1̄	*P*1̄	*P*1̄
a, Å	20.916 (3)	16.352 (5)	9.353 (1)	14.764 (3)
b, Å	19.361 (2)	15.169 (6)	15.114 (2)	9.574 (1)
c, Å	11.511 (2)	13.811 (4)	18.093 (3)	11.094 (2)
α, deg	90	99.06 (2)	88.41 (1)	87.26 (1)
β, deg	90	78.17 (2)	80.97 (1)	82.33 (2)
γ, deg	90	76.88 (3)	89.09 (1)	112.13 (1)
V, Å³	4661.3 (21)	3189.9 (19)	2524.8 (10)	1431.5 (5)
$F(000)$	2544	1472	1316	880
μ(Mo Kα), cm⁻¹	46.5	13.52	42.8	71.84
λ(Mo Kα), Å	0.71073	0.71069	0.71073	0.71069
monochromator	graphite	graphite	graphite	graphite
D_{calcd}, g cm⁻³	1.840	1.511	1.765	2.129
Z	4	2	2	2
no. of data $I > 3\sigma(I)$	3042	3201	4384	4035
R, %	3.2	7.8	3.3	6.7
octants measd	$+h,+k,+l$	$\pm h,+k,\pm l$	$+h,\pm k,\pm l$	$\pm h,+k,\pm l$
final no. of variables	295	803	640	353
diffractometer	Enraf-Nonius CAD/4	Syntex P₃	Enraf-Nonius CAD/4	Syntex P₃
T, °C	−110	+27	+20	+27

(24.38); Au, 21.46 (28.55); C, 26.19 (20.39); H, 1.96 (2.38); P, 3.38 (3.66).

X-ray Crystal Structures of [K(18-crown-6)][Fe₄(AuPEt₃)(CO)₁₃]·CH₂Cl₂ (3a) and [PPN][Fe₄(HgCH₃)(CO)₁₃] (6(tetrahedron)). Procedures and programs[25] described previously[26] were utilized during data collection, structure solution (heavy-atom methods), and refinement; details are summarized in Table I. The Au-containing compound was studied at about 163 K; a freshly grown crystal was mounted in air on a glass fiber and transferred immediately to the cold stream of an Enraf-Nonius CAD4 diffractometer. Systematic extinctions pointed to the space groups *Pnma* or *Pn2₁a*. The Patterson function was consistent with the centrosymmetric group *Pnma*, and subsequent refinement indicated that the mirror symmetry is imposed on the anion and the solvent molecule and the inversion symmetry imposed on the cation. Except within the triethylphosphine ligand, there are no abnormally large thermal parameters. Location of the H atoms of the cation and solvent molecule in difference Fourier maps provided further justification for the choice of the higher symmetry group. These H atoms were included as fixed contributions after idealization (r_{C-H} = 1.00 Å, B's 1 Å² greater than the B_{equiv} of the attached C atoms). The ethyl groups of the phosphine ligand, however, almost certainly do not conform to the mirror symmetry. The thermal parameters for the atoms in the ethyl groups (more accurately called anisotropic displacement parameters since it is unlikely that they describe "thermal" motion) are very large and the associated ellipsoids very eccentric. The bond lengths are short. Although the final difference Fourier function showed a number of peaks in the region of the ethyl groups, these peaks could not be assigned sensibly as H atoms. Undoubtedly these groups are disordered, and the refined coordinates correspond to averaged positions. There did not, however, seem to be any point in extending the model to try to account for the behavior of these peripheral ligands.

Crystals of the Hg-containing compound were sealed in thin-walled glass capillaries in an inert atmosphere and mounted on an Enraf-Nonius CAD4 diffractometer operating at room temperature. The H atoms of the PPN cation were included in the refinement as described above. The H atoms of the methyl group were not included in the refinement.

Single-Crystal X-ray Structure of [PPN][Fe₄(CuPPh₃)(CO)₁₃] (5a) and Fe₄AuPEt₃(CO)₁₂(COCH₃) (7). A crystal of [PPN][Fe₄Cu(PPh₃)-(CO)₁₃] (5a) and one of Fe₄(AuPEt₃)(CO)₁₂(COCH₃) (7) were sealed in individual capillaries and mounted on a Syntex P3 automated diffractometer. Unit cell dimensions (Table I) were determined by least-squares refinement of the best angular positions for 15 independent reflections (2θ > 15°) during normal alignment procedures using molybdenum radiation (λ = 0.71069 Å). Data (14691 (5a) and 9717 (7) points) were collected at room temperature with use of a variable scan rate, a θ–2θ scan mode, and a scan width of 1.2° below Kα₁ and 1.2° above Kα₂ to a maximum 2θ value of 55° for 5a and 64° for 7. Backgrounds were measured at each side of the scan for a combined time equal to the total scan time. The intensities of three standard reflections were remeasured after every 97 reflections and the intensities of these reflections showed less than 8% variation; therefore corrections for decomposition were deemed unnecessary. Data were corrected for Lorentz, polarization, and background effects. After removal of redundant data,

3201 (5a) and 4035 (7) reflections were considered observed [$I > 3.0\sigma$-(I)]. The structures were solved by direct methods using MULTAN80 to locate the heavy atoms.[27] Successive least-squares/difference Fourier cycles allowed location of the remainder of the non-hydrogen atoms. Refinement of scale factor and positional and anisotropic thermal parameters[28] for all non-hydrogen atoms was carried out to convergence. Hydrogen positional parameters were not determined. The final cycle of refinement function minimized [$\Sigma(||F_o| - F_c|)^2$] led to a final agreement factor, R = 7.8% (5a), 6.7% (7) [$R = (\Sigma||F_o| - |F_c||/\Sigma|F_o|)100$]. Anomalous dispersion corrections were made for Fe and Cu (5a) and Fe and Au (7). Scattering factors were taken from Cromer and Mann.[29] Units weights were used throughout.

Results and Discussion

Formation of [Fe₄(A)(CO)₁₃]⁻ Compounds. A 1:1 interaction is observed between [Fe₄(CO)₁₃]²⁻ and a variety of acceptors (eq 2). Adduct formation may be followed by infrared spectroscopy

$$[Fe_4(CO)_{13}]^{2-} + A^+ \rightarrow [Fe_4(A)(CO)_{13}]^- \qquad (2)$$
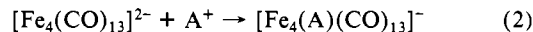
A = H; AuPR₃(R = Ph or Et);
CuL(L = PPh₃ or 2,6-(CH₃)₂C₆H₃NC); HgCH₃

(Table II) or color changes. The starting material is orange-brown and the color changes to red-brown upon addition of a proton acid, deep purple upon addition of Au and Cu Lewis acids, and red-purple for [CH₃Hg]⁺. IR spectra of the solutions show a 30–70 cm⁻¹ shift to higher energy for the strongest CO stretch relative to [Fe₄(CO)₁₃]²⁻ following adduct formation.

Methanol or CH₂Cl₂ solutions of the Au complexes are stable for hours in the absence of air, and solutions of the copper adduct show reasonable thermal stability when air is rigorously excluded. The mercury complex decomposes to [Fe₄(CO)₁₃]²⁻ when solutions are maintained at room temperature for more than 1 h. The most likely mercury-containing decomposition products are (CH₃)₂Hg and Hg metal. The redistribution reaction to form R₂Hg has been observed in other cluster systems.[30] Despite the instability in solution, the [CH₃Hg]⁺ complex of [Fe₄(CO)₁₃]²⁻ can be isolated as stable crystals. By changing the conditions for crystallization

(25) "Structure Determination Package"; B. A. Frenz and Associates: College Station, TX (Enraf-Nonius: Delft, Holland), 1982.

(26) Hrljac, J. A.; Swepston, P. N.; Shriver, D. F. *Organometallics* **1985**, *4*, 158.

(27) Main, P.; Fiske, S. J.; Hull, S. E.; Lessinger, L.; Germain, G.; DeClerg, J. P.; Woolfson, M. M., University of York, England 1980.

(28) Stewart, J. M. Ed. "The X-ray System-Version of 1980", Technical report TR446 of the Computer Center, University of Maryland, College Park, MD.

(29) Cromer, D. T.; Mann, I. B. *Acta Crystallogr. Sect. A* **1968**, *A24*, 321.

(30) Iggo, J. A.; Mays, M. J. *J. Chem. Soc., Dalton Trans.* **1984**, 643.

Table II. Infrared Stretching Frequencies[a]

	compound	CH$_2$Cl$_2$ soln	solid state[b]
1	[PPN]$_2$[Fe$_4$(CO)$_{13}$]	2018 w, 1943 vs	
2	[PPN][HFe$_4$(CO)$_{13}$]	2014 vs, 1989 s, 1970 m sh	2060 vw, 1985 vs, 1947 sh, 1829 w, *1416* w
3	[K(18-crown-6)][Fe$_4$(AuPR$_3$)(CO)$_{13}$] R = Et or Ph	2038 m, 1995 w sh, 1973 vs	2038 m, 1995 s sh, 1962 vs, 1928 vs, 1904 sh, 1880 sh *1412w* (1393 w R = Ph)
4	[PPN][Fe$_4$(AuPR$_3$)(CO)$_{13}$] R = Et or Ph	2038 m, 1971 vs, 1947 sh	2030 m, 1960 vs, 1939 s sh, 1908 s, 1890 sh, 1850 m, *1754 m*
5	[PPN][Fe$_4$(CuL)(CO)$_{13}$] L = PPh$_3$ or 2,6-(CH$_3$)$_2$C$_6$H$_3$NC	2036 w, 1997 sh, 1973 vs, 1910 br sh (ν_{N-C} 2160)	2030 m, 1981 s sh, 1962 vs, 1947, 1928 s sh, 1910 sh, 1889 s, 1865 m, br, *1729 w* br
6	[PPN][Fe$_4$(HgCH$_3$)(CO)$_{13}$] (butterfly)	2052 w, 2017 m, 1993 vs, 1965 sh	2052 w, 2009 vs, 1996 vs, 1972 vs, 1951 vs, 1930 vs, 1921 s, 1902 s, *1427* m
6	[PPN][Fe$_4$(HgCH$_3$)(CO)$_{13}$] (tetrahedron)	2052 w, 2017 m, 1993 vs, 1965 sh	2045 w, 1983 vs, 1952 w sh, 1941 w sh, 1935 m, 1920 w sh, 1834 w sh, *1820 w*
7	Fe$_4$(AuPEt$_3$)(CO)$_{12}$(COMe)	2072 w, 2037 vs, 2011 vs, 1988 s, sh 1920 w, sh	2074 w, 2040 vs, 2023 m, 2006 vs, 1988 s, 1967 m, 1941 w, 1932 w, 1905 w
8	HFe$_4$(CO)$_{12}$(COMe)[c]	2085 w, 2046 vs, 2020 s, 1998 s, 1990 m, 1890 w (hexane)	

[a] vs = very strong; s = strong; m = medium; w = weak; sh = shoulder; br = broad. [b] Fluorolube mull between KBr plates. [c] Reference 32.

Table III. Positional Parameters and Estimated Standard Deviations for [K(18-crown-6)][Fe$_4$(AuPEt$_3$)(CO)$_{13}$]·CH$_2$Cl$_2$[a]

atom	x	y	z
Au	0.15015 (2)	0.250	0.11746 (3)
Fe(1)	0.17753 (6)	0.250	0.4110 (1)
Fe(2)	−0.00768 (6)	0.250	0.3713 (1)
Fe(3)	0.09256 (4)	0.18159 (4)	0.28906 (7)
P	0.2091 (1)	0.250	−0.0489 (2)
C(10)	0.2312 (6)	0.1066 (4)	−0.0642 (9)
C(11)	0.2522 (5)	0.250	0.3261 (9)
C(12)	0.1917 (3)	0.1817 (3)	0.5104 (5)
C(13)	0.0895 (4)	0.250	0.4285 (7)
C(21)	−0.0373 (5)	0.250	0.2285 (8)
C(22)	−0.0575 (3)	0.1804 (4)	0.4214 (5)
C(31)	0.1661 (3)	0.1399 (3)	0.2672 (6)
C(32)	0.0566 (3)	0.1543 (3)	0.1562 (5)
C(33)	0.0643 (3)	0.1155 (3)	0.3808 (5)
O(11)	0.3004 (3)	0.250	0.2809 (7)
O(12)	0.1963 (2)	0.1380 (3)	0.5774 (4)
O(13)	0.0497 (3)	0.250	0.5099 (5)
O(21)	−0.0609 (3)	0.250	0.1374 (5)
O(22)	−0.0916 (2)	0.1378 (3)	0.4531 (4)
O(31)	0.2094 (2)	0.1028 (3)	0.2506 (4)
O(32)	0.0332 (2)	0.1315 (2)	0.0732 (4)
O(33)	0.0487 (3)	0.0708 (2)	0.4404 (4)

[a] Numbers in parentheses are estimated standard deviations in the least significant digits.
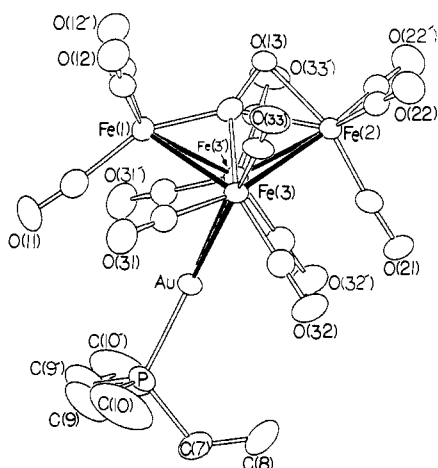
Figure 2. ORTEP diagram of [Fe$_4$(AuPEt$_3$)(CO)$_{13}$$^-$] (**3a**) with thermal ellipsoids at the 50% probability level. Carbonyl carbons are designated in a manner analogous to the oxygens to which they are attached.

two distinctly different forms of the [HgCH$_3$]$^+$ adduct can be isolated. One isomer, which has a butterfly iron core, is isolated when crystallization is rapid whereas the other isomer, with a tetrahedral iron core, is the product of slow crystallization. Examples of different isomers of clusters are known[31] but these

Table IV. Bond Distances (Å) and Angles (deg) for [K(18-crown-6)][Fe$_4$(AuPEt$_3$)(CO)$_{13}$]·CH$_2$Cl$_2$[a]

atom 1	atom 2	distance	atom 1	atom 2	distance
Au	Fe(3)	2.666 (1)	Fe(3)	C(13)	2.082 (6)
Au	P	2.278 (2)	Fe(3)	C(31)	1.756 (6)
Fe(1)	Fe(3)	2.623 (1)	Fe(3)	C(32)	1.784 (6)
Fe(2)	Fe(3)	2.654 (1)	Fe(3)	C(33)	1.761 (6)
Fe(3)	Fe(3′)	2.649 (2)	C(11)	O(11)	1.134 (9)
Fe(1)	C(11)	1.842 (9)	C(12)	O(12)	1.148 (7)
Fe(1)	C(12)	1.774 (7)	C(13)	O(13)	1.254 (9)
Fe(1)	C(13)	1.851 (9)	C(21)	O(21)	1.159 (9)
Fe(2)	O(13)	1.996 (5)	C(22)	O(22)	1.150 (7)
Fe(2)	C(13)	2.137 (9)	C(31)	O(31)	1.172 (7)
Fe(2)	C(21)	1.757 (9)	C(32)	O(32)	1.162 (7)
Fe(2)	C(22)	1.799 (7)	C(33)	O(33)	1.153 (7)

atom 1	atom 2	atom 3	angle
Fe(1)	Fe(3)	Fe(2)	95.31 (4)
Fe(3)	Au	Fe(3′)	59.57 (4)
Fe(3)	Au	P	150.18 (2)
Fe(3)	Fe(1)	Fe(3′)	60.64 (4)
Fe(3)	Fe(2)	Fe(3′)	59.86 (4)
Au	Fe(3)	Fe(1)	80.76 (3)
Au	Fe(3)	Fe(2)	111.92 (3)
Fe(1)	C(13)	Fe(2)	155.8 (4)
Fe(1)	C(11)	O(11)	175.2 (9)
Fe(1)	C(12)	O(12)	175.0 (6)
Fe(1)	C(13)	O(13)	137.9 (6)
Fe(2)	C(13)	O(13)	66.2 (4)
Fe(2)	O(13)	C(13)	78.6 (4)
Fe(2)	C(21)	O(21)	175.5 (8)
Fe(2)	C(22)	O(22)	176.9 (6)
Fe(3)	C(31)	O(31)	169.3 (6)
Fe(3)	C(32)	O(32)	174.7 (5)
Fe(3)	C(33)	O(33)	176.7 (6)

[a] Numbers in parentheses are estimated standard deviations in the least significant digits.

generally involve the disposition of CO ligands rather than gross changes in the metal framework. With the exception of [HFe$_4$(CO)$_{13}$]$^-$, all of the Lewis acid complexes of [Fe$_4$(CO)$_{13}$]$^{2-}$ are exceedingly difficult to recrystallize because they tend to expel the acceptor ligand or form oils.

Structural and Spectroscopic Characterization of [Fe$_4$(A)(CO)$_{13}$]$^-$ Species

(1) Fe$_4$ Butterfly Clusters. (a) Structure of [K(18-crown-6)][Fe$_4$(AuPEt$_3$)(CO)$_{13}$]·CH$_2$Cl$_2$ (**3a**). The molecular structure of the cluster anion [Fe$_4$(AuPEt$_3$)(CO)$_{13}$]$^-$ (**3a**) is shown in Figure 2. This view emphasizes both the butterfly geometry of the iron

(31) See, for example: (a) Garlaschelli, L.; Martinengo, S.; Bellon, P. L.; Demartin, F.; Manassero, M.; Chiang, M. Y.; Wei, C.-Y.; Bau, R. *J. Am. Chem. Soc.* **1984**, *106*, 6667. (b) Jackson, P. F.; Johnson, B. F. G.; Lewis, J.; McPartlin, M.; Nelson, W. J. H. *J. Chem. Soc., Chem. Commun.* **1978**, 920.
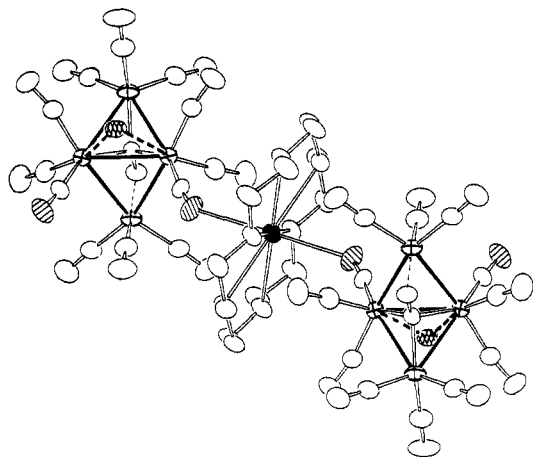
Figure 3. Diagram showing the cation–anion interactions for [K(18-crown-6)][$Fe_4(AuPEt_3)(CO)_{13}$]·CH_2Cl_2 (**3a**). The potassium is the solid sphere, carbonyls involved in Σ-CO formation are cross-hatched, the gold is doubly cross-hatched, and the irons are indicated by principle ellipses. The O(13)–Fe(2) interaction is the thin dashed line. The upper left cluster has the hinge coming out of the page while the lower right cluster has the Π-CO coming out of the page.

core as well as the presence of the Π-CO moiety. Crystal data, positional parameters, and derived bond distances and bond angles for complex **3a** are presented in Tables I, III, and IV respectively. The Fe–Fe distances in the butterfly complex **3a** range from 2.623 (1) to 2.654 (1) Å and average 2.642 (10) Å; these distances are similar to those in other butterfly compounds.[32] The Fe(3)–Fe(3′) distance, which corresponds to the hinge bond, is essentially identical with the Fe(2)–Fe(3) bond length, and both are significantly longer than the Fe(1)–Fe(3) distance. The lengthening of the Fe(2)–Fe(3) bond is most likely caused by the Π-interaction of Fe with the unique CO ligand. Interestingly, the presence of the PEt_3Au bridge across the hinge causes only a 0.03-Å increase in this Fe–Fe bond distance when compared to the analogous bond distance in [$HFe_4(CO)_{13}$]$^-$.[9a] This small increase appears to be common when Au replaces H.[33]

The semiface bridging disposition of the [Et_3PAu]$^+$ ligand in this cluster is unique. Thus the Au to Fe(3) and Fe(3′) distance, 2.665 (1) Å, is typical of gold to first-row transition metals, but the [Et_3PAu]$^+$ ligand is tipped toward a wingtip iron, with an Au–Fe(1) distance of 3.4 Å. It is possible that this weak Au–Fe(1) interaction arises because the Π-CO ligand serves as an electron acceptor toward the other wingtip iron, Fe(2), and therefore, the Fe(1)Fe(3)Fe(3′) face is more electron rich than the Fe(2)Fe(3)Fe(3′) face.

The disposition of terminal CO ligands in [$Fe_4(AuPEt_3)(CO)_{13}$]$^-$ is typical of the iron butterfly molecules. The Π-CO ligand in complex **3a** displays similar bond distances to the analogous [$HFe_4(CO)_{13}$]$^-$.[9] For example, the C–O distance for the Π-CO in **3a** is 1.248 (9) Å. The analogous bond length in the hydrido form is 1.254 (30) Å. Comparison of C–O distances in this Au-containing cluster shows a 0.10-Å increase in the C–O bond distance for the Π-CO vs. the average C–O distance of the terminal ligands. The Π-CO carbon, C(13), is closer to Fe(1), 1.851 (9) Å, than to Fe(2), 2.137 (9) Å, and the Fe(2) to O(13) distance is 1.996 (5) Å. In order to accommodate the oxygen, the butterfly opens to a dihedral angle of 117°. For iron butterflies with no group bridging the carbon–iron bond the dihedral angle is 10–15° smaller.[18,32]

As noted in the Experimental Section, a crystalline compound could not be isolated when either cryptands or dibenzo-18-crown-6 replaced 18-crown-6. A possible explanation for this lies in the orientation of the [K(18-crown-6)]$^+$ cation relative to the cluster anion. The potassium is coordinated to the six oxygens of the
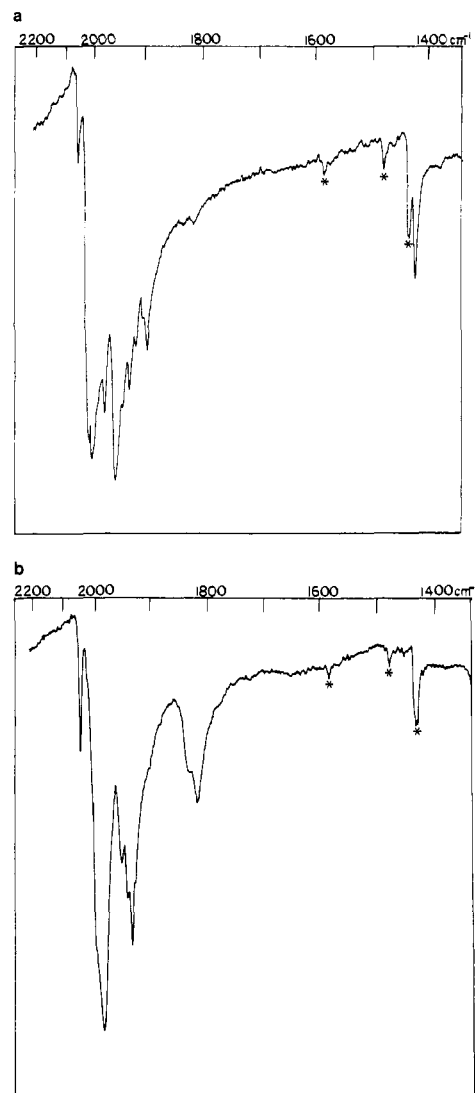
Figure 4. IR spectra of the two isomers of [$Fe_4(HgCH_3)(CO)_{13}$]$^-$ (**6**) as Fluorolube mulls between KBr plates: (a) Fe_4 butterfly; (b) Fe_4 tetrahedron; an asterisk denotes [PPN]$^+$ vibrations.

crown ether in a planar array, K–O distances of 2.747 (4) to 2.818 (4) Å, and also axially to two carbonyl oxygens O(32), K–O(32) = 2.770 (4) Å, of two independent anions thus forming a Σ-CO interaction Figure 3.[3,34] These interactions result in a stacking arrangement of both the cations and anions. The Σ-CO interaction is precluded for the cryptands by the encapsulation of the K$^+$, and for salts containing the dibenzo-18-crown-6 the phenyl rings might cause unfavorable steric interactions with CO ligands. The function of the CH_2Cl_2 is simply to fill voids created by this stacking arrangement.

(b) Spectroscopic Characterization. We have recently determined that the C–O stretch of the Π-CO in various salts of [$HFe_4(CO)_{13}$]$^-$ appears at approximately 1400 cm^{-1} in the IR spectrum[19] (Table II). This region of the IR spectrum is generally free of CO absorptions,[3] but absorption bands of the cation may be present. Thus labeling the cluster with ^{13}CO is necessary to definitively distinguish the Π-CO stretch from cation vibrations. For complex **3a**, which is established as a butterfly cluster with a Π-CO, a CO stretch in the mull IR spectrum is observed at 1412 cm^{-1} ($\nu(\Pi$-^{13}CO), 1380 cm^{-1}). Similarly for the rapidly crystallized form of [$Fe_4(HgCH_3)(CO)_{13}$]$^-$, **6**(butterfly), a low-frequency CO stretch occurs at 1427 cm^{-1} ($\nu(\Pi$-^{13}CO), 1393 cm^{-1}) (Figure 4a).

(32) Holt, E. M.; Whitmire, K. H.; Shriver, D. F. *J. Organomet. Chem.* **1981**, *213*, 125.

(33) Iggo, J. A.; Mays, M. J.; Raithby, P. R.; Henrick, K. *J. Chem. Soc., Dalton Trans.* **1984**, 633 and references therein.

(34) Coordination of a terminal carbonyl oxygen to an alkali metal of a crown ether has been observed previously. Cooper, M. K.; Duckworth, P. A.; Hendrick, K.; McPartlin, M. *J. Chem. Soc., Dalton Trans.* **1981**, 2357.
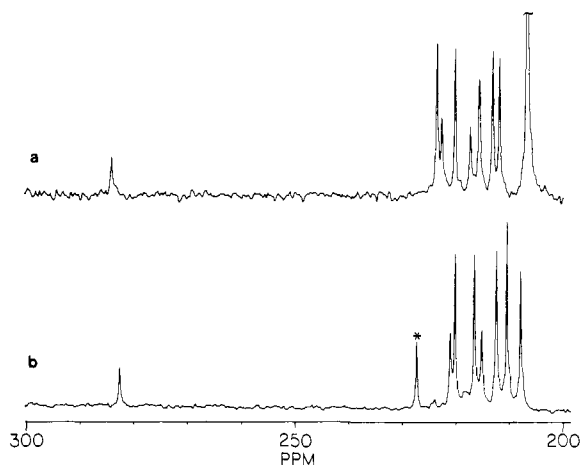
Figure 5. ^{13}C NMR spectra of (a) [Fe$_4$(AuPEt$_3$)(CO)$_{13}$]$^-$ (**3a**) and (b) [Fe$_4$(HgCH$_3$)(CO)$_{13}$]$^-$ (**6**(butterfly)) of the solids dissolved at -80 °C and the spectra recorded at this temperature. An asterisk denotes [Fe$_4$(CO)$_{13}$]$^{2-}$ impurity. The large upfield peak in part a is acetone solvent.

We found that the isomer observed in the solid state can be preserved in solution, by dissolving the solid at low temperature (-80 °C) and obtaining the NMR spectrum without ever allowing the sample to warm up.[12] In the following discussion we shall refer to spectra obtained in this manner simply as low-temperature spectra. In all instances the spectra are fully consistent with the structure in the solid state as determined by IR spectroscopy or X-ray crystallography.

Previous investigations[12,35] have shown that the resonance assignable to a Π-CO ligand in tetranuclear clusters is generally found in the 280–290 ppm region of the ^{13}C NMR spectrum. Shown in Figure 5 are the ^{13}C NMR spectra in the carbonyl region of [Fe$_4$(HgCH$_3$)(CO)$_{13}$]$^-$ (**6**(butterfly)) and [K(18-crown-6)]-[Fe$_4$(AuPEt$_3$)(CO)$_{13}$] (**3a**). In both instances solid samples were dissolved at -80 °C and the spectra were obtained at this temperature. Both complexes have downfield resonances owing to the Π-CO ligand and seven resonances in the terminal CO region which display intensity patterns consistent with the butterfly geometry, I (Table V). These spectra are in accord with the appearance of a low CO stretching frequency in the IR spectrum of both molecules (Table II) and the X-ray structural results for the Au complex.

I
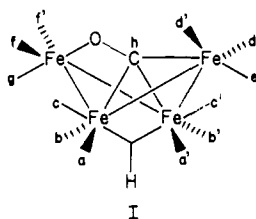
The low-temperature ^{31}P NMR spectra of the Au-containing complexes, **3**, display a single resonance (Table V). Although no structural information is available from these spectra, the variable-temperature NMR spectra discussed in the accompanying paper[7] indicate that the position of the single resonances is characteristic of the Fe$_4$ butterfly isomer. That is, the structure observed in the solid state persists in solution.

The ^{199}Hg{^{1}H} NMR spectrum of the butterfly compound [Fe$_4$(HgCH$_3$)(CO)$_{13}$]$^-$, **6**(butterfly), shows a resonance at 1353 ppm downfield of a 0.1 M CDCl$_3$ solution of CH$_3$HgCl. This resonance is shifted significantly downfield. For example, it is 500–700 ppm downfield of (CH$_3$)$_2$Hg. The ^{199}Hg NMR spectra of compounds of the type [CpM(CO)$_3$]$_2$Hg (M = Cr, Mo, or W)[36]

(35) Brun, P.; Dawkins, G. M.; Green, M.; Miles, A. D.; Orpen, A. G.; Stone, F. G. A. *J. Chem. Soc., Chem. Commun.* **1982**, 926.
(36) Albright, M. J.; Oliver, J. P. *J. Organomet. Chem.* **1979**, *172*, 99.

Table V. ^{13}C and ^{31}P NMR Spectroscopic Data^{a,b}

compd	^{13}C{^{1}H}	^{31}P{^{1}H}	solvent
1	227.8		CD$_2$Cl$_2$
2	279.8 (1); 221.5 (2)		
	219.7 (1); 217.5 (1)		CD$_2$Cl$_2$
	215.6 (2); 211.4 (2)		
	209.5 (2); 209.1 (2)		
3a	284.6 (1); 224.0 (2)		(CD$_3$)$_2$CO
	223.1 (1); 220.6 (2)	57.7	
	217.8 (1); 216.1 (2)		
	213.5 (2); 212.4 (2)		
3b	284.7 (1); 224.0 (2)		
	223.0 (1); 220.9 (2)	58.3	(CD$_3$)$_2$CO
	218.4 (1); 215.6 (2)		
	213.3 (2); 212.0 (2)		
4a	222.0	57.8 (22.2 [PPN]$^+$)	CD$_2$Cl$_2$
4b	221.7	56.8 (22.2 [PPN]$^+$)	CD$_2$Cl$_2$
5a	220.7	3.03 (broad)	CD$_2$Cl$_2$
5b	220.4		CD$_2$Cl$_2$
6 (butterfly)	282.6 (1); 221.1 (1)		CD$_2$Cl$_2$
	220.9 (2); 216.5 (2)		
	215.1 (1); 212.4 (2)		
	210.5 (2); 207.9 (2)		
7	303.5 (1); 219.9 (2)	58.1	CD$_2$Cl$_2$
	216.1 (2); 214.3 (1)		
	212.8 (2); 211.3 (1)		
	208.3 (2); 207.5 (2)		
8	301 (1); 217.5 (2)		CD$_2$Cl$_2$
	212.4 (2); 211.3 (2)		
	210.8 (2); 209.9 (2)		
	206.9 (2)		

^{a} External references: ^{13}C, SiMe$_4$, and ^{31}P, 85% H$_3$PO$_4$. ^{b} Values in parentheses refer to relative intensities. ^{c} Spectra of solid samples dissolved and run at -80 °C.
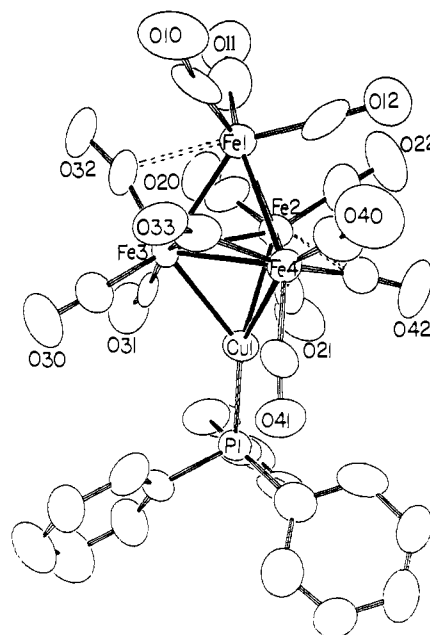
Figure 6. ORTEP diagram of [Fe$_4$(CuPPh$_3$)(CO)$_{13}$]$^-$ (**5a**) with thermal ellipsoids at the 50% probability level. Carbonyl carbons are designated in a manner analogous to the oxygens to which they are attached.

also display downfield mercury resonances. The $^2J_{^1H-^{199}Hg}$ coupling constant for the proton-coupled spectrum of **6** is 134 Hz. This value is relatively small when compared to other CH$_3$HgX compounds[37,38] and suggests that the mercury to iron bonding is rather covalent.

(37) Rabenstein, D. L. *Acc. Chem. Res.* **1978**, *11*, 100.
(38) (a) Hatton, J. V.; Schneider, W. G.; Siebrand, W. *J. Chem. Phys.* **1963**, *39*, 1330. (b) Sytsma, L. F.; Kline, R. J. *J. Organomet. Chem.* **1973**, *54*, 15. (c) Canty, A. J.; Marker, A. *Inorg. Chem.* **1976**, *15*, 425. (d) Rabenstein, D. L.; Tourangeau, M. C.; Evans, C. A. *Can. J. Chem.* **1976**, *54*, 2517. (e) Henneike, H. F. *J. Am. Chem. Soc.* **1972**, *94*, 5945.

Formation of II-CO Ligands in Four-Iron Clusters

J. Am. Chem. Soc., Vol. 107, No. 26, 1985 8143

Table VI. Positional Parameters and Estimated Standard Deviations for [PPN][Fe$_4$(CuPPh$_3$)(CO)$_{13}$]

atom	x	y	z
Cu(1)	0.6387 (2)	0.1770 (2)	0.6851 (2)
Fe(1)	0.8177 (2)	0.0792 (3)	0.8458 (3)
Fe(2)	0.7833 (2)	0.0600 (3)	0.6701 (3)
Fe(3)	0.7332 (2)	0.2234 (2)	0.7966 (3)
Fe(4)	0.6567 (2)	0.0970 (2)	0.8339 (3)
P(1)	0.5428 (4)	0.2387 (5)	0.6060 (5)
P(2)	0.0775 (4)	0.4433 (5)	0.2513 (5)
P(3)	0.1852 (4)	0.3640 (4)	0.0377 (4)
N(1)	0.1072 (12)	0.4108 (15)	0.1337 (13)
O(10)	0.8400 (14)	0.1244 (16)	1.0495 (15)
O(11)	1.0024 (12)	0.0187 (15)	0.7561 (16)
O(12)	0.8092 (12)	-0.1093 (14)	0.8523 (15)
O(20)	0.9381 (13)	0.1073 (15)	0.5759 (18)
O(21)	0.7449 (15)	0.0562 (14)	0.4740 (14)
O(22)	0.8661 (17)	-0.1369 (14)	0.6094 (18)
O(30)	0.6354 (15)	0.4090 (13)	0.9077 (18)
O(31)	0.7600 (15)	0.2962 (15)	0.6149 (15)
O(32)	0.8909 (12)	0.2610 (13)	0.8417 (14)
O(33)	0.6543 (10)	0.2310 (13)	1.0149 (12)
O(40)	0.6046 (15)	0.0138 (17)	1.0037 (17)
O(41)	0.4742 (10)	0.1879 (13)	0.8555 (13)
O(42)	0.6474 (14)	-0.0659 (15)	0.6962 (19)
C(10)	0.8279 (17)	0.1131 (18)	0.9690 (20)
C(11)	0.9260 (20)	0.0465 (20)	0.7938 (20)
C(12)	0.8094 (16)	-0.0303 (22)	0.8516 (20)
C(20)	0.8770 (19)	0.0912 (22)	0.6214 (21)
C(21)	0.7485 (16)	0.0653 (16)	0.5556 (16)
C(22)	0.8351 (22)	-0.0579 (21)	0.6310 (23)
C(30)	0.6729 (17)	0.3343 (17)	0.8638 (20)
C(31)	0.7462 (18)	0.2611 (16)	0.6817 (19)
C(32)	0.8340 (16)	0.2314 (17)	0.8234 (18)
C(33)	0.6768 (15)	0.1882 (18)	0.9297 (17)
C(40)	0.6223 (15)	0.0430 (17)	0.9368 (18)
C(41)	0.5474 (15)	0.1556 (16)	0.8416 (17)
C(42)	0.6645 (18)	-0.0022 (19)	0.7366 (23)
C(111)	0.4978 (16)	0.3633 (17)	0.6600 (19)
C(112)	0.4855 (18)	0.3912 (22)	0.7632 (20)
C(113)	0.4482 (22)	0.4844 (21)	0.8090 (25)
C(114)	0.4274 (21)	0.5508 (20)	0.7562 (23)
C(115)	0.4411 (25)	0.5224 (26)	0.6489 (28)
C(116)	0.4782 (21)	0.4248 (23)	0.5990 (29)
C(121)	0.4483 (17)	0.1968 (18)	0.6168 (16)
C(122)	0.4543 (18)	0.1010 (22)	0.6225 (21)
C(123)	0.3789 (22)	0.0688 (22)	0.6251 (28)
C(124)	0.3027 (20)	0.1250 (20)	0.6255 (22)
C(125)	0.2935 (20)	0.2173 (21)	0.6239 (20)
C(126)	0.3630 (17)	0.2561 (20)	0.6227 (20)
C(131)	0.5809 (18)	0.2268 (19)	0.4697 (19)
C(132)	0.6558 (19)	0.2505 (23)	0.4277 (18)
C(133)	0.6861 (19)	0.2304 (23)	0.3245 (19)
C(134)	0.6442 (23)	0.1964 (22)	0.2586 (24)
C(135)	0.5669 (24)	0.1760 (22)	0.2983 (23)
C(136)	0.5304 (18)	0.1942 (19)	0.4071 (19)

**(2) Fe$_4$ Tetrahedral Clusters. (a) Structures of [PPN][Fe$_4$-(CuPPh$_3$)(CO)$_{13}$] (5a) and [PPN][Fe$_4$(HgCH$_3$)(CO)$_{13}$] (6(tetrahedron)).** The molecular structures of the Fe$_4$ tetrahedral complexes [Fe$_4$(CuPPh$_3$)(CO)$_{13}$]$^-$ (5a) and [Fe$_4$(HgCH$_3$)(CO)$_{13}$]$^-$ (6(tetrahedron)) are shown in Figures 6 and 7. For both clusters, the Lewis acid ligand caps one of the triangular faces of the tetrahedron. Crystal data for both complexes are found in Table I. Positional parameters are presented in Tables VI and VII for 5a and 6, respectively, while derived distances and angles are given in Tables VIII (5a) and IX (6). The average Fe–Fe bond distances of 2.606 (11) and 2.627 (15) Å for complexes 5a and 6, respectively, are comparable to the M–M distances in the 14-CO cluster [Fe$_3$Cr(CO)$_{14}$]$^{2-}$,[10] but longer than the 2.54 to 2.58 Å normally observed in 13-ligand tetrahedral iron clusters.[39] The variation in Fe–Fe bond lengths within the two clusters is considerable, see Tables VIII and IX. These differences are caused
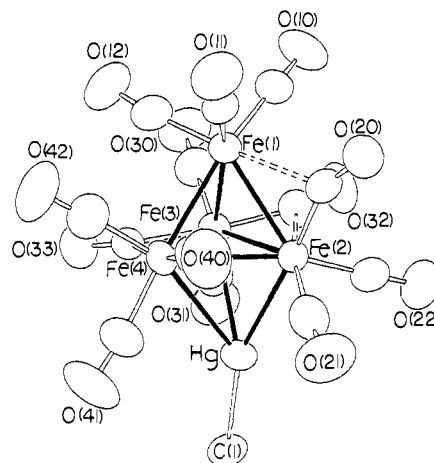
Figure 7. ORTEP diagram of [Fe$_4$(HgCH$_3$)(CO)$_{13}$]$^-$ (6(tetrahedron)) with thermal ellipsoids at the 50% probability level. Carbonyl carbons are designated in a manner analogous to the oxygens to which they are attached.

Table VII. Positional Parameters and Their Estimated Standard Deviations for [PPN][Fe$_4$(HgCH$_3$)(CO)$_{13}$][a]

atom	x	y	z
Hg	0.30774 (3)	0.21981 (2)	0.16121 (2)
Fe(1)	0.6470 (1)	0.22840 (7)	0.31140 (6)
Fe(2)	0.4712 (1)	0.31288 (7)	0.23289 (6)
Fe(3)	0.3903 (1)	0.16385 (7)	0.30020 (6)
Fe(4)	0.5981 (1)	0.15858 (7)	0.18754 (6)
O(10)	0.5865 (6)	0.2941 (4)	0.4652 (3)
O(11)	0.9488 (5)	0.2855 (4)	0.2783 (3)
O(12)	0.7304 (7)	0.0548 (4)	0.3671 (4)
O(20)	0.6696 (6)	0.4333 (4)	0.2839 (3)
O(21)	0.5311 (7)	0.4015 (5)	0.0873 (3)
O(22)	0.2625 (7)	0.4561 (4)	0.2673 (4)
O(30)	0.3831 (7)	0.0760 (5)	0.4458 (3)
O(31)	0.0949 (6)	0.1046 (4)	0.3022 (4)
O(32)	0.2836 (6)	0.3131 (4)	0.3931 (3)
O(33)	0.4745 (6)	-0.0151 (4)	0.2491 (3)
O(40)	0.8047 (6)	0.2862 (4)	0.1121 (4)
O(41)	0.5391 (7)	0.0818 (5)	0.0490 (3)
O(42)	0.8373 (7)	0.0334 (5)	0.1864 (4)
C(1)	0.1627 (8)	0.1931 (6)	0.0847 (4)
C(10)	0.6104 (8)	0.2699 (5)	0.4054 (4)
C(11)	0.8298 (8)	0.2641 (6)	0.2894 (4)
C(12)	0.6944 (8)	0.1208 (6)	0.3430 (5)
C(20)	0.6067 (7)	0.3709 (5)	0.2724 (4)
C(21)	0.5092 (8)	0.3628 (6)	0.1431 (5)
C(22)	0.3395 (8)	0.3975 (6)	0.2542 (4)
C(30)	0.3916 (9)	0.1099 (6)	0.3881 (5)
C(31)	0.2114 (8)	0.1290 (5)	0.2974 (5)
C(32)	0.3390 (8)	0.2688 (6)	0.3449 (4)
C(33)	0.4757 (8)	0.0618 (5)	0.2509 (4)
C(40)	0.7158 (8)	0.2423 (5)	0.1449 (4)
C(41)	0.5564 (8)	0.1150 (6)	0.1023 (4)
C(42)	0.7432 (9)	0.0836 (6)	0.1898 (5)

[a] Numbers in parentheses are estimated standard deviations in the least significant digits.

primarily by the presence of bridging and semibridging CO ligands.

The Cu–Fe distances in 5a are fairly symmetrical, 2.525 (6) to 2.580 (6) Å, and are similar to bond lengths between Cu and other first-row transition metals.[24,40] The Hg complex shows rather asymmetric bonding of the mercury to the three basal iron atoms. The Hg–Fe(2) distance is 2.606 (1) Å and the other two Hg to Fe distance are longer (Hg–Fe(3) = 2.847 (1) Å and Hg–Fe(4) = 2.960 (1) Å). This contrasts with the relatively symmetric bonding of the face capping (CO)$_4$CoHg[41a] moiety to

(39) Horwitz, C. P.; Holt, E. M.; Shriver, D. F. *Organometallics* **1985**, *4*, 1117.

(40) Churchill, M. R.; Bezman, S. A.; Osborn, J. A.; Wormald, J. *Inorg. Chem.* **1972**, *11*, 1818.

Table VIII. Bond Distances (Å) and Angles (deg) for [PPN][Fe$_4$(CuPPh$_3$)(CO)$_{13}$][a]

atom 1	atom 2	distance	atom 1	atom 2	distance
Cu(1)	Fe(2)	2.562 (5)	Fe(1)	C(32)	2.44 (3)
Cl(1)	Fe(3)	2.526 (5)	Fe(2)	C(42)	2.42 (3)
Cu(1)	Fe(4)	2.579 (5)	Fe(3)	C(33)	2.09 (2)
Cu(1)	P(1)	2.211 (8)	Fe(4)	C(42)	1.81 (3)
Fe(1)	Fe(2)	2.588 (6)	Fe(4)	C(33)	1.89 (3)
Fe(1)	Fe(3)	2.576 (5)	C(32)	O(32)	1.18 (4)
Fe(1)	Fe(4)	2.627 (6)	C(33)	O(33)	1.19 (3)
Fe(2)	Fe(3)	2.645 (5)	C(42)	O(42)	1.16 (4)
Fe(3)	Fe(4)	2.576 (6)	Cu(1)	C(21)	2.38 (2)
Fe(4)	Fe(2)	2.621 (5)	Cu(1)	C(31)	2.39 (3)
Fe(1)	C(33)	2.44 (2)	Cu(1)	C(41)	2.47 (2)

atom 1	atom 2	atom 3	angle	atom 1	atom 2	atom 3	angle
Fe(2)	Cu(1)	Fe(3)	62.6 (1)	Cu(1)	Fe(4)	Fe(3)	58.7 (1)
Fe(2)	Cu(1)	Fe(4)	61.3 (1)	Fe(2)	Fe(1)	Fe(3)	61.6 (1)
Fe(3)	Cu(1)	Fe(4)	60.6 (2)	Fe(2)	Fe(1)	Fe(4)	60.3 (1)
Fe(2)	Cu(1)	P(1)	147.0 (2)	Fe(3)	Fe(1)	Fe(4)	59.4 (2)
Fe(3)	Cu(1)	P(1)	140.6 (3)	Fe(2)	Fe(3)	Fe(4)	60.2 (1)
Fe(4)	Cu(1)	P(1)	143.6 (3)	Fe(3)	Fe(4)	Fe(2)	61.2 (1)
Cu(1)	Fe(2)	Fe(1)	108.3 (2)	Fe(4)	Fe(2)	Fe(3)	58.6 (1)
Cu(1)	Fe(3)	Fe(1)	109.8 (2)	Fe(1)	C(32)	O(32)	124 (2)
Cu(1)	Fe(4)	Fe(1)	106.6 (2)	Fe(3)	C(32)	O(32)	162 (2)
Cu(1)	Fe(2)	Fe(3)	58.0 (1)	Fe(3)	C(33)	O(33)	130 (2)
Cu(1)	Fe(2)	Fe(4)	59.7 (1)	Fe(1)	C(33)	O(33)	127 (2)
Cu(1)	Fe(3)	Fe(2)	59.4 (1)	Fe(4)	C(33)	O(33)	146 (2)
Cu(1)	Fe(3)	Fe(4)	60.7 (1)	Fe(2)	C(42)	O(42)	126 (2)
Cu(1)	Fe(4)	Fe(2)	59.0 (1)	Fe(4)	C(42)	O(42)	159 (2)

[a] Numbers in parentheses are estimated standard deviations in the least significant digits.

Table IX. Bond Distances (Å) and Angles (deg) for [PPN][Fe$_4$(HgCH$_3$)(CO)$_{13}$][a]

atom 1	atom 2	distance	atom 1	atom 2	distance
Hg	Fe(2)	2.606 (1)	Fe(1)	C(20)	2.292 (7)
Hg	Fe(3)	2.847 (1)	Fe(2)	C(20)	1.800 (7)
Hg	Fe(4)	2.960 (1)	Fe(2)	C(32)	2.290 (8)
Hg	C(1)	2.134 (6)	Fe(3)	C(32)	1.823 (9)
Fe(1)	Fe(2)	2.630 (1)	Fe(3)	C(33)	1.905 (8)
Fe(1)	Fe(3)	2.645 (1)	Fe(4)	C(33)	2.077 (8)
Fe(1)	Fe(4)	2.610 (1)	C(20)	O(20)	1.160 (7)
Fe(2)	Fe(3)	2.597 (1)	C(32)	O(32)	1.166 (8)
Fe(2)	Fe(4)	2.689 (1)	C(33)	O(33)	1.164 (8)
Fe(3)	Fe(4)	2.589 (1)			

atom 1	atom 2	atom 3	angle	atom 1	atom 2	atom 3	angle
Fe(2)	Hg	Fe(3)	56.67 (3)	Fe(2)	Fe(1)	Fe(4)	61.77 (3)
Fe(2)	Hg	Fe(4)	57.36 (3)	Fe(3)	Fe(1)	Fe(4)	59.03 (3)
Fe(3)	Hg	Fe(4)	52.91 (3)	Fe(1)	Fe(2)	Fe(3)	60.80 (3)
Fe(2)	Hg	C(1)	157.9 (2)	Fe(1)	Fe(2)	Fe(4)	58.76 (3)
Fe(3)	Hg	C(1)	143.3 (2)	Fe(3)	Fe(2)	Fe(4)	58.62 (3)
Fe(4)	Hg	C(1)	137.1 (2)	Fe(1)	Fe(3)	Fe(2)	60.21 (3)
Hg	Fe(2)	Fe(1)	118.31 (4)	Fe(1)	Fe(3)	Fe(4)	59.81 (3)
Hg	Fe(2)	Fe(3)	66.36 (3)	Fe(2)	Fe(3)	Fe(4)	62.48 (4)
Hg	Fe(2)	Fe(4)	67.96 (3)	Fe(1)	Fe(4)	Fe(2)	59.48 (3)
Hg	Fe(3)	Fe(1)	109.81 (4)	Fe(1)	Fe(4)	Fe(3)	61.16 (3)
Hg	Fe(3)	Fe(2)	56.97 (3)	Fe(2)	Fe(4)	Fe(3)	58.91 (3)
Hg	Fe(3)	Fe(4)	65.79 (3)	Fe(1)	C(20)	O(20)	126.8 (5)
Hg	Fe(4)	Fe(1)	107.44 (4)	Fe(2)	C(20)	O(20)	154.2 (6)
Hg	Fe(4)	Fe(2)	54.68 (3)	Fe(2)	C(32)	O(32)	128.0 (6)
Hg	Fe(4)	Fe(3)	61.31 (3)	Fe(3)	C(32)	O(32)	154.6 (7)
Fe(2)	Fe(1)	Fe(3)	58.99 (3)	Fe(4)	C(33)	O(33)	133.6 (6)
				Fe(3)	C(33)	O(33)	145.5 (7)

[a] Numbers in parentheses are estimated standard deviations in the least significant digits.

[RuCo$_3$(CO)$_{12}$]$^-$. The iron–mercury distances are on average longer than those previously observed between Hg and other first-row transition metals.[41] The asymmetric bonding arrangement of the CH$_3$Hg moiety may reflect the high propensity of CH$_3$Hg to adopt a linear two-coordinate geometry.[37]

The disposition of CO ligands in clusters **5a** and **6**(tetrahedron) is similar. For both clusters terminal CO ligands have M–C–O bond angles ranging from 165° to 179°, M–C distances of 1.7

(41) (a) Braunstein, P.; Rose, J.; Tiripicchio, A.; Tiripicchio-Camellini, M. *J. Chem. Soc., Chem. Commun.* **1984**, 391. (b) Bryan, R. F.; Weber, H. P. *Acta Crystallogr. Sect. A* **1966**, *21*, 138. (c) Sheldrick, G. M.; Simpson, R. N. F. *J. Chem. Soc. A* **1968**, 1005. (d) Duffy, D. N.; Mackay, K. M.; Nicholson, B. K.; Robinson, W. T. *J. Chem. Soc., Dalton Trans.* **1981**, 381.

to 1.8 Å, and C–O distances of 1.1 to 1.2 Å. Each cluster has one edge-bridging CO in the basal plane, C(33)–O(33), which in the case of the Cu complex **5a** is also tipped toward the apical iron and may be described as semiface bridging. The Cu complex has two semibridging CO ligands, C(42)–O(42) and C(32)–O(32), which bridge a basal edge, Fe(2)–Fe(4), and a basal-apical edge, Fe(1)–Fe(3), respectively. For [Fe$_4$(HgCH$_3$)(CO)$_{13}$]$^-$, the semibridging ligands are C(32)–O(32) and C(20)–O(20) with the former bridging the Fe(1)–Fe(2) edge and the latter bridging the Fe(2)–Fe(3) bond.

(b) Spectroscopic Characterization. The infrared spectra of complexes **5a** and **6**(tetrahedron) in the solid state show the presence of a bridging CO at 1729 and 1820 cm^{-1}, respectively,

Scheme II

4: A= AuPR$_3$

5: A= CuL
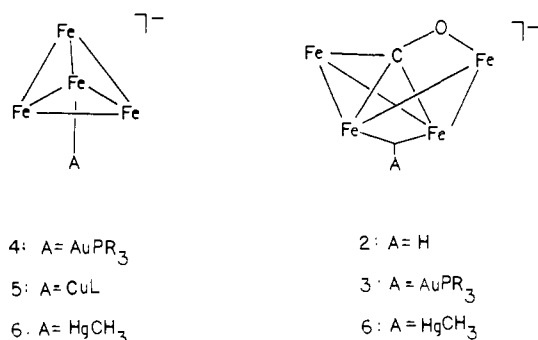
6: A= HgCH$_3$

2: A= H

3: A = AuPR$_3$

6: A = HgCH$_3$

Table II, consistent with the presence of the edge-bridging CO observed in the X-ray structure of both compounds. The solid-state IR spectrum of $[Fe_4(HgCH_3)(CO)_{13}]^-$ (6(tetrahedron)) is shown in Figure 4b. Comparison of this spectrum with the butterfly form of this cluster anion, Figure 4a, clearly reveals the absence of the low-frequency CO stretch of the II-CO ligand. The IR spectrum of $[PPN][Fe_4(AuPR_3)(CO)_{13}]$ (4) in the solid state displays an absorption at 1754 cm^{-1} for a bridging CO but no band in the 1400-cm^{-1} region (Table II). Thus changing the cation from $[K(18\text{-crown-6})]^+$ (3) to $[PPN]^+$ (4) appears to change the cluster geometry from a Fe$_4$ butterfly in 3 to a Fe$_4$ tetrahedron in 4. The NMR spectra of 4, described below, confirm the tetrahedral geometry of the iron core.

For the NMR spectra discussed below, all of the sample were prepared by dissolving the isolated crystalline solid at -80 °C and then obtaining the spectrum at this temperature. When the tetrahedral complex $[Fe_4(CuPPh_3)(CO)_{13}]^-$ (5a) is prepared in this manner, a single resonance in the carbonyl region is observed in the ^{13}C NMR spectrum (Table V). Rapid CO exchange over the metal framework appears to be a characteristic property of the anionic Fe$_4$ tetrahedral clusters. Similarly, $[PPN][Fe_4-(AuPR_3)(CO)_{13}]$ (4) produces a ^{13}C NMR spectrum with only a single sharp resonance for the solid dissolved at -80 °C and the spectrum obtained at this temperature (Table V). This result supports the assignment of a Fe$_4$ tetrahedron for this compound inferred from the IR spectroscopic data described above. These observations strengthen our previous assignment of the feature at 216.7 ppm in the ^{13}C NMR spectrum of $[HFe_4(CO)_{13}]^-$ to a tetrahedral isomer.[12]

The ^{31}P NMR spectrum of a sample of 4 dissolved and run at -80 °C shows the presence of only a single downfield resonance. A direct comparison with the spectrum obtained for the butterfly form of this anion 3 is not possible since solubility differences between complexes 3 and 4 required the use of different solvents. However, the variable-temperature spectra described in the following paper[7] are consistent with a tetrahedral geometry for complex 4.

Interesting comparisons can be made between the ^{199}Hg NMR spectra for the two isomers of $[Fe_4(HgCH_3)(CO)_{13}]^-$ (6). As previously noted, the butterfly form shows a resonance at 1353 ppm. For the tetrahedral isomer a shift to even lower field occurs and the resonance appears at 1449 ppm. Comparison of the $^2J_{^1H-^{199}Hg}$ coupling constants also is interesting. This coupling constant for the butterfly isomer is 134 Hz, and for the tetrahedral isomer it is 146 Hz. The slightly larger coupling constant observed for the face-capping CH$_3$Hg moiety in the tetrahedron vs. the edge bridge for the butterfly is consistent with the approximate four coordination for the Hg in the former complex.[37,38] Scheme II summarizes the structures for the various compounds observed in the solid state, as determined by X-ray structural data and the various spectroscopic data discussed above. Interestingly, we have no indication from any of these data for the Lewis acid bridging the edge of the iron tetrahedron (Scheme I). However, this species might be an intermediate in the interconversion of the butterfly and face-capped tetrahedral isomers.

(3) Reaction of $[Fe_4(CO)_{12}(COMe)]^-$ with PEt$_3$AuCl. The conversion of a tetrahedral cluster with a Σ-CO to a II-CO

Table X. Positional Parameters and Estimated Standard Deviations for $Fe_4(AuPEt_3)(CO)_{12}(COCH_3)$

atom	x	y	z
Au(1)	0.7214 (1)	0.4660 (1)	0.6973 (1)
Fe(1)	0.7793 (2)	0.6669 (3)	1.0383 (2)
Fe(2)	0.8566 (2)	0.5835 (2)	0.8407 (2)
Fe(3)	0.7093 (2)	0.6826 (2)	0.8345 (2)
Fe(4)	0.8784 (2)	0.8195 (3)	0.6897 (2)
P(1)	0.6622 (4)	0.2870 (5)	0.5683 (5)
O(99)	0.8870 (8)	0.8629 (12)	0.9536 (10)
C(98)	0.8868 (14)	1.0154 (18)	0.9595 (22)
C(99)	0.8495 (11)	0.7827 (17)	0.8600 (15)
O(10)	0.6187 (12)	0.3714 (16)	0.0947 (16)
O(11)	0.6792 (12)	0.7937 (20)	1.2239 (16)
O(12)	0.8954 (14)	0.5838 (23)	1.2013 (15)
O(20)	0.7692 (12)	0.2584 (15)	0.9355 (17)
O(21)	1.0408 (9)	0.6662 (14)	0.9371 (14)
O(22)	0.9636 (11)	0.5227 (21)	0.6216 (15)
O(30)	0.6241 (11)	0.8813 (16)	0.9540 (15)
O(31)	0.6606 (11)	0.7748 (17)	0.6056 (14)
O(32)	0.5157 (9)	0.4244 (16)	0.8769 (15)
O(40)	1.0917 (11)	0.9519 (23)	0.6909 (21)
O(41)	0.8694 (14)	0.7331 (20)	0.4351 (14)
O(42)	0.8702 (13)	1.1138 (18)	0.6435 (20)
C(10)	0.6802 (16)	0.4854 (23)	1.0683 (20)
C(11)	0.7171 (14)	0.7473 (21)	1.1495 (18)
C(12)	0.8520 (16)	0.6192 (25)	1.1371 (18)
C(20)	0.7999 (13)	0.3857 (20)	0.8993 (19)
C(21)	0.9668 (12)	0.6331 (16)	0.9021 (15)
C(22)	0.9178 (14)	0.5494 (23)	0.7022 (18)
C(30)	0.6597 (13)	0.8022 (19)	0.9046 (18)
C(31)	0.6890 (12)	0.7405 (19)	0.6892 (17)
C(32)	0.5925 (13)	0.5197 (20)	0.8613 (19)
C(40)	1.0102 (17)	0.9026 (31)	0.6864 (23)
C(41)	0.8699 (16)	0.7616 (23)	0.5369 (20)
C(42)	0.8733 (15)	0.9973 (24)	0.6607 (21)
C(111)	0.7596 (16)	0.2878 (28)	0.4456 (20)
C(112)	0.7231 (23)	0.1750 (40)	0.3531 (27)
C(121)	0.5650 (16)	0.3086 (27)	0.4897 (22)
C(122)	0.6003 (18)	0.4558 (30)	0.4097 (22)
C(131)	0.6093 (18)	0.0927 (21)	0.6469 (24)
C(132)	0.5300 (20)	0.0762 (26)	0.7627 (29)

butterfly compound is observed when $[Fe_4(CO)_{12}(COMe)]^-$ reacts with either the proton[22,42] or a $[AuPEt_3]^+$ moiety, eq 3. Reaction

$$[Fe_4(CO)_{12}(COMe)]^- + A^+ \rightarrow Fe_4A(CO)_{12}(COMe) \quad (3)$$
$$\Sigma\text{-CO–Me} \qquad\qquad\qquad\qquad \Pi\text{-CO–Me}$$

$$A = H^+ \text{ or } [AuPEt_3]^+$$
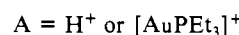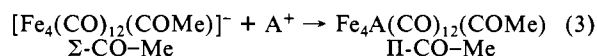
of the red-black $K[Fe_4(CO)_{12}(COMe)]$ cluster with the gold–phosphine in toluene results in a color change to green–black. The infrared spectrum of the product, $Fe_4(AuPEt_3)(CO)_{12}(COMe)$ (Table II) is similar to the hydrido analogue with all bands shifted to lower energy for the Au complex.

(a) Structure of $Fe_4(AuPEt_3)(CO)_{12}(COMe)$. The molecular structure of this compound, 7, was determined by a single-crystal X-ray structure, and the result is shown in Figure 8. Crystal data are presented in Table I, final positional parameters are given in Table X, and derived distances and angles can be found in Table XI. Structurally, the hydride[32] and gold–phosphine complexes are very similar. Aside from the length of the Fe–Fe hinge bond which is 2.605 (1) Å for the hydride acceptor and 2.687 (4) Å for the AuPEt$_3$ acceptor, all Fe–Fe distances are essentially the same within experimental error. The slight, 0.08 Å, increase on changing the acceptor from H$^+$ to $[AuPEt_3]^+$ is similar to that observed for the analogous bonds in $[Fe_4(AuPEt_3)(CO)_{13}]^-$ (3) and $[HFe_4(CO)_{13}]^-$. Comparison of the C–O distance in this II-CO–Me compound, C(99)–O(99) = 1.37 (2) Å, with the analogous bond in $[HFe_4(CO)_{13}]^-$ and $[Fe_4(AuPEt_3)(CO)_{13}]^-$, shows an increase on the order of 0.1 Å. The II-CO–Me group is bonded asymmetrically between the wingtip irons with Fe-(1)–C(99) being 2.14 (2) Å whereas Fe(4)–C(99) is 1.86 (2) Å.

---

(42) Whitmire, K. H.; Shriver, D. F. *J. Am. Chem. Soc.* **1981**, *103*, 6754.

Figure 8. ORTEP diagram of $Fe_4(AuPEt_3)(CO)_{12}(COCH_3)$ (7) w... thermal ellipsoids at the 50% probability level. Carbonyl carbons are designated in a manner analogous to the oxygens to which they are attached. The methyl carbon of the Π-CO–CH_3 group is labeled as C98.

Table XI. Bond Distances (Å) and Angles (deg) for $Fe_4(AuPEt_3)(CO)_{12}(COCH_3)^a$

atom 1	atom 2	distance
Au(1)	Fe(2)	2.666 (2)
Au(1)	Fe(3)	2.675 (3)
Au(1)	P(1)	2.278 (5)
Fe(1)	Fe(2)	2.632 (4)
Fe(1)	Fe(3)	2.629 (4)
Fe(2)	Fe(3)	2.687 (4)
Fe(2)	Fe(4)	2.638 (4)
Fe(3)	Fe(4)	2.606 (3)
Fe(1)	C(99)	2.14 (2)
Fe(2)	C(99)	1.97 (2)
Fe(3)	C(99)	1.99 (2)
Fe(4)	C(99)	1.86 (2)
Fe(1)	O(99)	2.029 (9)
C(99)	O(99)	1.37 (2)
C(98)	O(99)	1.46 (2)

atom 1	atom 2	atom 3	angle
Fe(2)	Au(1)	Fe(3)	60.40 (8)
Fe(1)	Fe(3)	Fe(4)	97.81 (11)
Fe(1)	Fe(2)	Fe(4)	96.95 (12)
Fe(2)	Au(1)	P(1)	146.5 (2)
Fe(3)	Au(1)	P(1)	152.8 (2)
Au(1)	Fe(2)	Fe(1)	110.99 (10)
Au(1)	Fe(3)	Fe(1)	110.80 (11)
Au(1)	Fe(2)	Fe(4)	76.75 (8)
Au(1)	Fe(3)	Fe(4)	77.14 (9)
Fe(2)	Fe(1)	Fe(3)	61.42 (9)
Fe(2)	Fe(4)	Fe(3)	61.63 (9)
Fe(1)	Fe(2)	Fe(3)	59.24 (10)
Fe(1)	Fe(3)	Fe(2)	59.34 (10)
Fe(4)	Fe(2)	Fe(3)	58.60 (9)
Fe(4)	Fe(3)	Fe(2)	59.77 (9)
Fe(1)	C(99)	Fe(4)	159.5 (8)
C(99)	O(99)	C(98)	119 (2)

^{a} Numbers in parentheses are estimated standard deviations in the least significant digits.

Comparison of these distances with $[Fe_4(AuPEt_3)(CO)_{13}]^-$ (Table IV) shows that the presence of the CH_3 group does not affect the orientation of the carbon of the Π-CO between the butterfly wingtips. Thus the dihedral angle of 122° observed in this cluster is similar to that of **3**. Addition of the CH_3 group to the Π-CO oxygen has only a minimal effect on the oxygen to wingtip iron distance. This bond length is 2.000 (2) Å in $HFe_4(CO)_{12}(CO-CH_3)$,[32] 2.029 (9) Å in $Fe_4(AuPEt_3)(CO)_{12}(COCH_3)$, 1.996 (5) Å in $[Fe_4(AuPEt_3)(CO)_{13}]^-$, and 2.00 Å in $[HFe_4(CO)_{13}]^{-}.$[9a]

Furthermore, the molybdenum–oxygen distance of 2.17 Å in $Cp^*_2Mo_2Fe_2(CO)_{11}$[43] is nearly the same as these oxygen–iron distances when compensation is made for the larger radius of molybdenum. The insensitivity of the metal–oxygen bond length to the presence of a methyl group is somewhat surprising in view of the significant effect on the C–O bond length of the Π-CO. As with complex **3**, the $AuPEt_3$ moiety is bent away from the iron wingtip bonded to the Π-CO–Me (3.3 Å from Fe(1) and 3.9 Å from Fe(2)). In the hydrido form the proton appears to be symmetrically disposed between the two wingtip iron atoms. This similarity between the two Au-containing clusters lends credence to the idea that the bending of the $AuPEt_3$ moiety in the hinge position toward one of the triangular iron faces arises from the presence of the Π-CO rather than simple crystal packing forces.

(b) Spectroscopic Characterization. The low-temperature (−90 °C) ^{13}C NMR spectrum has a Π-CO–Me resonance at 303.5 ppm and a series of resonances in the terminal CO region (Table V). Variable-temperature NMR data indicate a unique fluxionality pattern of carbonyl ligands in comparison with other butterfly clusters.[44] In this instance it appears that the carbonyl ligands on Fe(1) do not participate in either an exchange or a rotational process. Furthermore, the remaining CO ligands appear to undergo several exchange processes among the three remaining iron vertices. We are unable to definitely determine the fluxionality pattern because it is not possible to unambiguously assign the CO resonances in the low-temperature spectrum. Nevertheless the presence of the Π-CO-Me group has a significant influence on CO exchange in this cluster. The unique fluxionality observed in the ^{13}CO NMR spectrum is not the result of confusion with a second isomer in solution because ^{31}P NMR spectroscopy indicates the presence of only one isomer.[7]

(4) Conclusion. The formation of Π-CO ligands is induced in $[Fe_4(CO)_{13}]^{2-}$ by the attachment of electron-acceptor ligands to the metal core. Similarly, a cluster containing the Σ-CO–Me ligand, $[Fe_4(CO)_{12}(COMe)]^-$, is converted to a butterfly cluster with a Π-CO–Me group upon addition of a Lewis acid ligand to the metal framework. Apparently, acceptor ligands not only decrease the overall charge on the cluster but also have a marked effect on details of the metal–metal bonding within the cluster. These results as well as the work of others[45] suggest that electron acceptor ligands might be more generally applied in metal cluster chemistry to alter the geometry of the metal framework.

Supplementary Material Available: Tables of full positional parameters, thermal parameters, and bond distances and angles for $[K(18$-crown-$6)][Fe_4(AuPEt_3)(CO)_{13}]$ and $[PPN][Fe_4(Hg-CH_3)(CO)_{13}]$ (errors were found in the previously deposited bond distance and angle table for $[PPN][Fe_4(CuPPh_3)(CO)_{13}]$; a new corrected table is available) (19 pages). Ordering information is given on any current masthead page.

(43) (a) Gibson, C. P.; Mahood, J. A.; Huang, J. S.; Dahl, L. F. "Abstracts of Papers", 187th National Meeting of the American Chemical Society, St. Louis, MO; American Chemical Society: Washington, D.C., April 1984; INOR 202. (b) The CO bond distance of the Π-CO ligand is 1.17 Å.

(44) (a) Beno, M. A.; Williams, J. M.; Tachikawa, M.; Muetterties, E. L. *J. Am. Chem. Soc.* **1981**, *103*, 1485. (b) Tachikawa, M.; Muetterties, E. L. *J. Am. Chem. Soc.* **1980**, *102*, 4541. (c) Evans, J.; Johnson, B. F. G.; Lewis, J.; Matheson, T. W. *J. Am. Chem. Soc.* **1975**, *97*, 1245.

(45) (a) McPartlin, M.; Eady, C. R.; Johnson, B. F. G.; Lewis, J. *J. Chem. Soc., Chem. Commun.* **1976**, 883. (b) Braga, D.; Henrick, K.; Johnson, B. F. G.; Lewis, J.; McPartlin, M.; Nelson, W. J. H.; Vargas, M. D. *Ibid.* **1982**, 419. (c) Johnson, B. F. G.; Lewis, J.; Nelson, W. J. H.; Raithby, P. R.; Vargas, M. D. *Ibid.* **1983**, 608. (d) Puga, J.; Sanchez-Delgado, R.; Andriollo, A.; Ascanio, J.; Braga, D. *Organometallics*, submitted.